ACCUMULATING ENERGY IN ASSISTIVE SPRINGS USING BOUNDED FORCE AND DEFORMATION: THEORY, MECHANISM DESIGN, AND EXPERIMENTAL VALIDATION

By

Cole Dempsey

Thesis

Submitted to the Faculty of the

Graduate School of Vanderbilt University

in partial fulfillment of the requirements

for the degree of

MASTER OF SCIENCE

in

MECHANICAL ENGINEERING

December 17th, 2022

Nashville, Tennessee

Approved:

David Braun, Ph.D.

Nilanjan Sarkar, Ph.D.

Michael Goldfarb, Ph.D.

ACKNOWLEDGMENTS

I would like to express my gratitude to my advisor Dr. David Braun, Vanderbilt University, and the Department of Mechanical Engineering for the opportunity to do advanced research and earn my graduate degree in a field I'm deeply passionate about. I also greatly appreciate the support and expertise provided by my entire thesis committee: Dr. Nilanjan Sarkar and Dr. Michael Goldfarb. I am especially thankful for my fellow lab mates, who provided endless encouragement and guidance throughout my graduate experience. Most importantly, I would like to thank my family for their unwavering support and belief in my goals. Words cannot adequately describe how meaningful the constant love from back home was to my success.

TABLE OF CONTENTS

LIST OF FIGURES

CHAPTER 1

Overview

1.1 Introduction and Motivation

Wearable assistive devices, such as exoskeletons and exosuits, have continued to evolve as a promising technology to help able-bodied users walk and run more efficiently, bear heavier loads, and complete tasks with greater endurance. Several trends in exoskeleton design have emerged to accomplish these goals, however, research in this area is faced with the same fundamental challenge: the strategic use of energy in the human-wearable system [1]. On one hand, active exoskeletons utilize electrical power to provide motorized assistance to the joints of the user with great adaptability to changing task conditions, but rely on substantial power supplies that limit functionality and effective use time [1].

Alternatively, passive and quasi-passive exoskeleton devices have found success as a way to circumvent this power supply barrier. These devices store energy from the negative work performed during many common tasks, such as the deceleration of the lower-limbs during late swing into stance during walking or running [2, 3] or the stooping over of the upper-body to grab an object [4], by placing elastic elements in series or parallel with the joints of the user. The stored elastic potential is then utilized to assist in positive work phases of the motion, for example, to assist with ankle-plantarflexion during push-off while walking [5], often utilizing clutched elastic actuation techniques to efficiently control energy storage and release [6].

While placing elastic elements in conjunction with human joints can enhance peak power output [7], especially when utilized with variable stiffness implementations [8], this process accomplishes only a bounded reduction in user effort since the assistance passive mechanisms can provide is limited by the amount of negative work performed by the user during a single motion cycle. As humans we are physiologically limited in our ability to do work, due to our limited range of motion and force output, which places a constraint on the amount of energy one can store and utilize in passive elastic elements of assistive exoskeletons during a single motion cycle.

To extend the benefit of assistive springs, the work outlined in this document contributes a method and mechanism that allows a user, with a bounded static potential, to accumulate considerable energy in assistive springs over several motion cycles. Specifically, this work explores foundational theory for cyclic energy accumulation by repeated squatting with a lower-limb exoskeleton. The iterative squat-to-stand task serves as a representative example of cyclic energy accumulation in assistive springs subject to the aforementioned physiological constraints. The challenges of such a task are investigated through a model of a novel variable

stiffness spring transmission, and used to inform the design of an initial prototype. By equipping wearable assistive devices with the ability to accumulate energy with a limited force, this technology has the potential to expand the capabilities of passive assistive devices beyond the current limits imposed by constrained force and range of motion.

1.2 Organization of the Document

This thesis is organized into four distinct chapters. Chapter 1 introduces the background literature and motivation driving this work. In Chapter 2, the body of this work is presented via a conference paper that was submitted to the International Conference on Robotics and Automation (ICRA) as a culmination of the research performed for this thesis. This paper details the foundational theory, prototype design, and experimental validation investigated to accomplish cyclic energy accumulation under physiological constraints as introduced in Chapter 1. Next, Chapter 3 delves further into how the energy accumulation method can be applied to enhance physical performance, such as jumping ability. Finally, Chapter 4 provides deeper insight into the design of the prototype to inform future work, along with closing discussion of this research.

CHAPTER 2

Manuscript: Novel Spring Mechanism Enables Iterative Energy Accumulation under Force and Deformation Constraints

Cole A. Dempsey and David J. Braun

Vanderbilt University

Nashville, Tennessee

Submitted as a Conference Paper to the

IEEE International Conference on Robotics and Automation

(In Review)

2.1 Abstract

Springs can provide force at zero net energy cost by recycling negative mechanical work to benefit motor-driven robots or spring-augmented humans. However, humans have limited force and range of motion, and motors have a limited ability to produce force. These limits constrain how much energy a conventional spring can store and, consequently, how much assistance a spring can provide. In this paper, we introduce an approach to accumulating negative work in assistive springs over several motion cycles. We show that, by utilizing a novel floating spring mechanism, the weight of a human or robot can be used to iteratively increase spring compression, irrespective of the potential energy stored by the spring. Decoupling the force required to compress a spring from the energy stored by a spring advances prior works, and could enable spring-driven robots and humans to perform physically demanding tasks without the use of large actuators.

2.2 Introduction

Springs can enable robots actuated by motors [7, 9, 10, 11, 12, 13] and humans “actuated by muscles" [14, 15, 5, 16, 8, 17, 18, 19] to perform physically demanding tasks with reduced force requirements from the actuators. In most applications, a spring is compressed slowly over a longer period of time, while the energy stored by the spring is released rapidly [20]. In this way, the spring provides power amplification beyond what a motor driven robot or “muscle actuated" human can do without the assistance of a spring. However, the energy stored by a spring is limited by the maximum force used to compress the spring. Consequently, the maximal force that a robot or human can generate limits the amount of energy a spring can store, and the level of assistive benefit a spring can provide. This limitation may be alleviated by leveraging the energy storage ability of springs over multiple loading and unloading cycles instead of a single cycle.

In mechanical resonance, the benefit of springs is leveraged over multiple cycles of energy storage and release, instead of a single cycle [21, 22, 23, 24, 25, 26]. A familiar example is a pogo-stick, essentially a spring in series with the human legs, that allows the user to jump repeatedly to accumulate energy and reach jump heights much greater than in a single jump [27]. To accomplish such a feat, the pogo-stick relies on iteratively increasing the kinetic energy of the human through multiple jumps. This increase in kinetic energy is required to generate the large contact forces to compress the pogo-stick spring and thereby increase the energy stored by the spring. However, large forces are challenging for humans and robots to generate without increasing their kinetic energy.

In this paper, we present a method and a device for iteratively accumulating energy using only the static gravitational force provided by the mass of a spring-driven robot or the mass of a human augmented with a spring leg exoskeleton. The method utilizes the repeated application of a constant static force that is independent of the energy stored by the spring. The method also relies on a new device, which belongs to

the class of floating spring mechanisms recently introduced in [28]. The device is an energetically passive variable stiffness spring which automatically adjusts its stiffness to ensure that a constant force can compress the spring regardless of how much energy is stored by the spring.

The working principle of the device is demonstrated using a point mass model of the human squatting with a lower-limb spring leg exoskeleton in Section 2.3. The energy accumulation method is subsequently described in Section 2.4. Then, the prototype of the device is detailed in Section 2.5. Finally, the experimental validation of the proposed energy accumulation method is reported in Section 2.6.

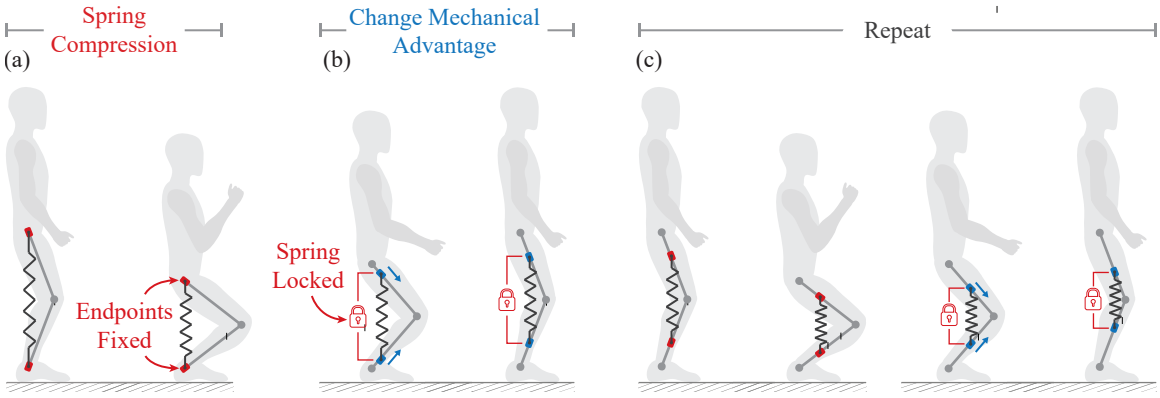

Figure 2.1: Repeated squatting with a floating variable stiffness spring. (a) The end points of the spring are fixed (red) while the user compresses the spring with a squat. (b) The end points of the spring are free (blue) while the spring is locked. The mechanical advantage of the human over the spring is increased as the human stands and the spring shifts towards the knee joint. (c) By repeating the energy accumulation cycle (a)-(b), the user can iteratively increase the energy stored by the spring.

2.3 Energy Accumulation using Springs

Let us consider a simple energy accumulation task where the human is augmented with a spring exoskeleton attached parallel to the legs, see Fig. 2.1. In this task, the user compresses the spring by repeatedly squatting with the exoskeleton. The energy stored by the spring is retained by locking the spring at the bottom of each squat. As the human returns to the standing height, the spring shifts to a new configuration that grants the user a greater mechanical advantage over the spring for the next iteration. The greater mechanical advantage ensures the user can compress the spring at the beginning of each squat cycle until a desired amount of energy is accumulated in the spring. In the described iterative energy accumulation process, the force required by the human to achieve full spring compression is independent of the energy stored by the spring.

In the remainder of this section, we further explore the example squatting task using a simple spring mass model of the human augmented with a conceptual lower-limb variable stiffness spring exoskeleton.

2.3.1 Model

The human and the spring-leg exoskeleton are abstracted into the model shown in Fig. 2.2a. We consider a single squat, starting from an upright standing position and ending at the fully squatted position. Due to the geometric constraint of the leg, the leg deformation during a squat is given by

$$\Delta l \in [0, \Delta l_{\max}]. \tag{2.1}$$

Because the human leg can push but cannot pull against the ground while squatting, the force exerted by the leg on the center of mass must be positive,

$$F \geq 0. \tag{2.2}$$

Finally, we assume that the human legs can produce enough force to stand up after each squat without the support of the exoskeleton. Any leg force that can overcome the weight of the human $F \geq mg$ suffices this assumption.

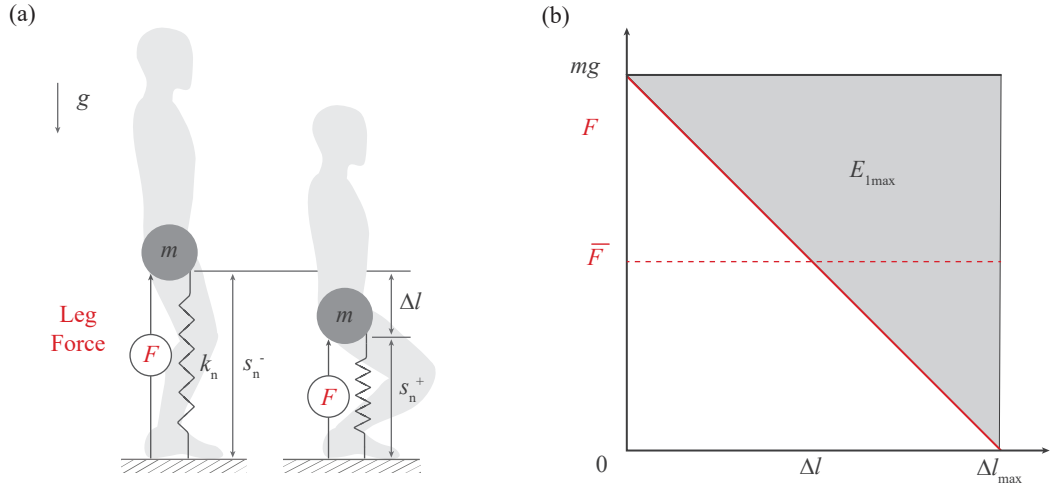

Figure 2.2: Model of the human augmented with a lower-limb exoskeleton. (a) Mass-spring system. The leg deformation is described by Δl. The body mass is supported by a spring with stiffness k_n and deformed length $s_n^{\pm}$; the superscripts $\pm$ denote the pre-squat and post-squat spring lengths, respectively, and the subscript n denotes the number of squats performed during repeated squatting. (b) An example force-deflection of the human leg F (red) that leads to the average leg force $\bar{F} = \frac{1}{2}mg$ is shown with the red line. The maximum amount of energy accumulated during one squat $E_{1\max}$ is shown with the dark area.

An example of the human leg force that enables squatting from a standing position to the equilibrium position is shown in Fig. 2.2b. At standing the human limbs fully support the mass such that $F = mg$ and the spring-leg exoskeleton does not provide any force. In the fully squatted position, the human limbs may support the mass with a force $F \in [0, mg)$ while the spring leg provides the rest of the force required to keep

the center of mass in static equilibrium,

$$mg = F + k\Delta l_{\max}. \tag{2.3}$$

At the bottom of the squat, the energy stored by the spring leg depends on the human limb force. Assuming an average limb force $\bar{F}$, the energy stored by the spring is given by:

$$\frac{1}{2}k\Delta l_{\max}^2 = (mg - \bar{F})\Delta l_{\max}. \tag{2.4}$$

In order to simultaneously satisfy (2.3) and (2.4), the average force of the human leg $\bar{F}$ during the squat must satisfy the following condition:

$$\bar{F} = \frac{1}{2}(mg + F). \tag{2.5}$$

According to (2.4) and (2.5), the maximum amount of energy that can be stored in the spring during a single squat is given by:

$$E_{1\max} = \frac{1}{2}mg\Delta l_{\max}, \tag{2.6}$$

Relation (2.6) directly shows that the amount of energy accumulated in the spring is restricted by the range of motion and the limited gravitational force available to compress the spring. In the next section, we introduce a novel spring mechanism that can alleviate the aforementioned limitation.

2.4 Cyclic Energy Accumulation by a Floating Spring Variable Stiffness Leg

There are three main practical challenges of realizing energy accumulation beyond a single squat:

(i) The mechanism must provide increased mechanical advantage to compress the spring, such that the same force can be used to compress the spring even as it stores more energy.

(ii) The mechanism must provide controllable coupling between the spring and the leg, such that the same leg deformation can be used to input energy into the spring in subsequent squats independent of how much energy is stored by the spring.

(iii) To ensure efficient energy accumulation, the two prior tasks should be accomplished while maintaining the energy stored in the spring between subsequent iterations.

In order to address the aforementioned challenges, a special case of the floating spring mechanism proposed in [28] is presented (Fig. 2.3). In the original design, the mechanical advantage of the human over the

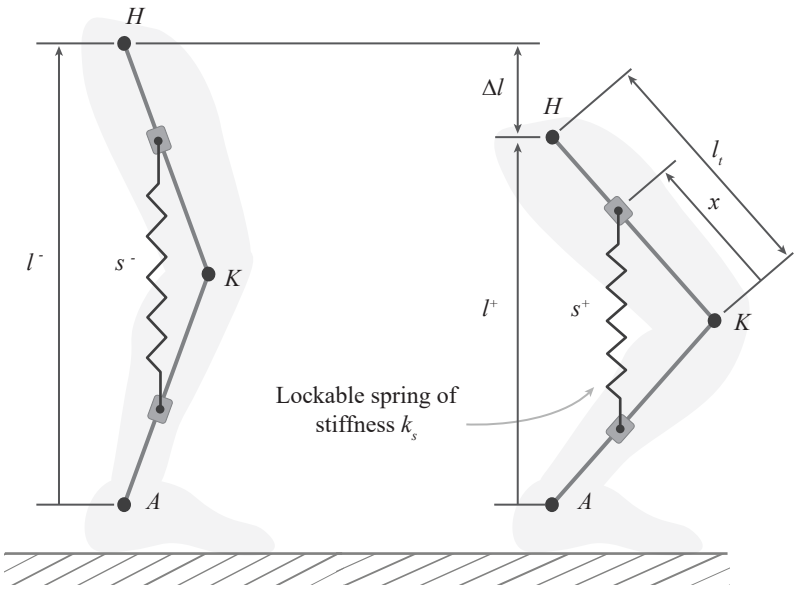

Figure 2.3: Model of the variable stiffness floating spring-leg. The leg segments $\overline{HK}$ and $\overline{KA}$ are equal in length. The spring is assumed to remain vertical (x is constant) as the leg deforms by Δl.

spring was manipulated by changing the orientation of the spring. In the proposed design, the spring maintains a vertical orientation but shifts towards or away from the knee joint to change the mechanical advantage. Due to this difference, the proposed design always maintains positive force-deflection behavior. Both designs, however, alter mechanical advantage by controlling the endpoints of the spring while the spring is locked, which maintains the potential energy stored by the spring. In turn, this ability to control the endpoints of the spring allows the leg deformation to be decoupled from the spring deformation, independent of the energy stored by the spring. Consequently, the proposed design addresses all three of the practical challenges (i)-(iii) mentioned above.

In what follows, we present the geometry that grants the spring leg mechanism energetically efficient variable stiffness behavior (Section 2.4.1), and describe the working principle of the mechanism (Section 2.4.2) consistent with the three main requirements outlined above.

2.4.1 Model

Figure 2.3 shows the floating spring variable stiffness leg for a single squat iteration. In the leg, points H, K and A coincide with the user's hip, knee, and ankle, respectively. The thigh and shank segments $\overline{HK}$ and $\overline{KA}$ are assumed to be of equal length l_t. The spring is also assumed to maintain its vertical orientation independent of the leg deformation. In the mechanism, the length of the spring s is defined by leg length l

and the position of the spring x,

$$s = \frac{x}{l_t} l, \tag{2.7}$$

while the force required at the hip F_l to compress the spring is defined by,

$$F_l = \left(\frac{x}{l_t}\right) F_s = \left(\frac{x}{l_t}\right) k_s (s_0 - s), \tag{2.8}$$

where s_0 is the uncompressed length of the spring and k_s is the stiffness of the spring.

These relations suggest that by moving the spring towards the knee joint – decreasing x – a small constant force F_l could be used at the hip to compress the spring despite a potentially large spring force F_s, and consequently, the large amount of energy stored by the spring.

The next section explores how the mechanism shown in Fig. 2.3 could accumulate a large amount of energy when compressed by the weight of the human over multiple squats.

2.4.2 Cyclic Energy Accumulation

In order to predict the behavior of the mechanism beyond a single squat, we again consider the simple example of a human performing a repetitive squat task to accumulate energy in the spring as introduced in Section 2.3.

First, similar to (2.3), we assume that the spring-leg supports the weight of the user at the end of each squat,

$$mg = k_s \left(\frac{x_n}{l_t}\right) \left(s_0 - s_n^+\right). \tag{2.9}$$

To define the spring length at the end of the squat s_n^+, the spring location x_n must be related to the spring length at the beginning of the squat s_n^-. The simple relation below follows from locking the spring length between the end of the previous squat and the beginning of the next squat (Fig. 2.1),

$$s_{n-1}^+ = s_n^-. \tag{2.10}$$

According to (2.10), the energy stored by the spring will be retained between squats,

$$\frac{1}{2} k_s \left(s_{n-1}^+ - s_0\right)^2 = \frac{1}{2} k_s \left(s_n^- - s_0\right)^2. \tag{2.11}$$

Finally, using (2.7) and (2.10), we define a recurrence relation that predicts the position of the spring across squat iterations:

$$x_n = \frac{\bar{s_n}}{\bar{s_{n-1}}} x_{n-1}. \tag{2.12}$$

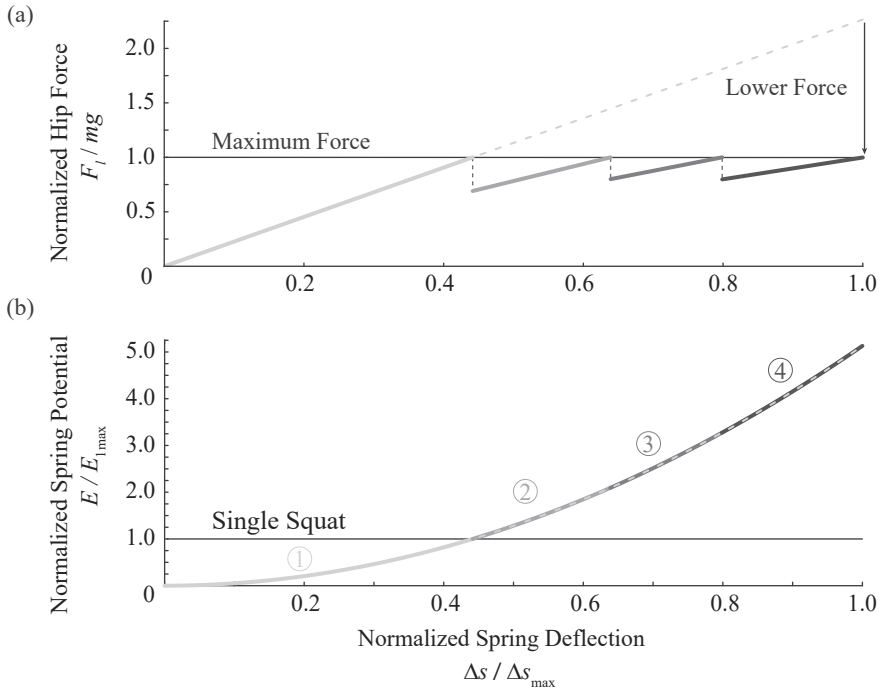

Figure 2.4: Simulated behavior for the spring-leg. (a) Force-deflection achieved by repeated squats, subject to a limited force (horizontal line), compared to the force required to achieve the same deformation in a single compression cycle (dashed line). The forces are normalized by the weight of the user (Section 2.3.1). (b) Potential energy stored by the spring, normalized by the max amount of energy that can be accumulated in a single squat $E_{1\max}$ (2.6) defined in (Section 2.3.1). The four squats shown in the figure were the minimum number of squats necessary to achieve full spring deformation.

Substituting (2.9), (2.10), and (2.12) into (2.8), we find that the force required to compress the spring at the beginning of the next squat is always lower than the constant gravitational force available to compress the spring,

$$F_{ln}^{-} = \left(\frac{\bar{s_n}}{\bar{s_{n-1}}} \right) mg \;\leq\; mg. \tag{2.13}$$

Figure 2.4a shows the force-deflection predicted during multiple squats, during which the maximal force provided by the human is bounded by the weight of the user (gray). This force is compared to the force required to achieve the same spring deformation in a single squat (gray dashed). Further, the vertical dashed

lines show that the spring deformation is maintained between iterations, as required by (2.10).

Figure 2.4b shows the energy accumulation process for the iterative method (gray), with energetic potential normalized by the maximum energy that can be achieved in a single squat provided by the weight of the user, $E_{1\max}$, as defined in (2.6).

We observe that the spring accumulates the same amount of energy through four squats (gray) than in a single squat (gray dashed) but with less than half of the required force (Fig. 2.4a-b). Furthermore, we observe that the reduction in force translates to over five times more stored energy as compared to what can be accumulated in a single squat subject to the same maximum force (Fig. 2.4b). Following the repeated squats, the spring can be reset to the initial mechanical advantage, $x = l_t$, where the accumulated energy can be released to provide double the assistive force as compared to the maximal force used to compress the spring (Fig. 2.4a) and the energy stored by the spring when compressed with the maximal force in a single squat (Fig. 2.4b).

2.5 Prototype

In this section, a prototype of the floating spring mechanism introduced in Section 2.4 is presented.

2.5.1 Device

Figure 2.5 depicts the spring-leg prototype designed for the proposed energy accumulation task. The device consists of three major sub-assemblies: the leg structure, the compression spring, and the spring retraction mechanism. These sub-assemblies are detailed below.

First, the leg structure is formed by two linear shafts connected by brackets at the knee and pinned to create a hinge joint. The other ends of each shaft form the hip and ankle of the mechanism, as in Fig. 2.3.

Second, a compression spring is housed in a piston-cylinder assembly where each endpoint of the assembly connects to a linear ball bearing that slides freely along the leg shafts. To lock the spring axially, a shoulder bolt passes orthogonally through a hole in the piston and rides in a slot in the cylinder, as shown in Fig. 2.5a. The cylinder features flat sides as an interface for the shoulder bolt, allowing continuous locking of the spring.

Finally, two uni-directional pulleys, each with two drums, are mounted in coincidence with the knee joint pin, as shown in Fig. 2.5b. One pulley is keyed to the knee pin, while the other pulley spins freely on the knee pin. Both, however, can spin freely with respect to the knee brackets. The two drums on each pulley feature separate cables wrapped in opposing directions. One cable connects to an extension spring that provides a torque on the pulley, while the other cable is connected to an endpoint of the spring assembly. The system of pulleys serves to automatically shift the position of the spring assembly, and consequently change the

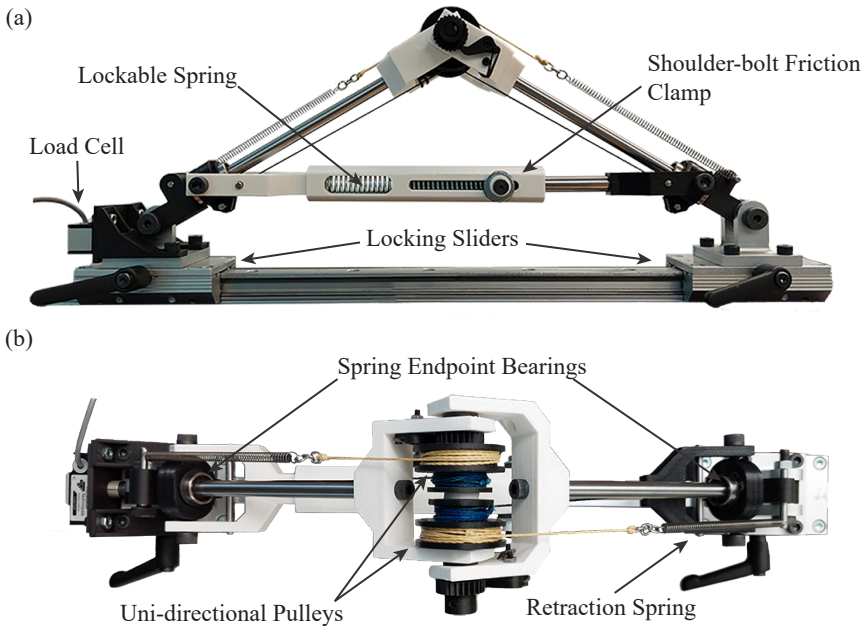

Figure 2.5: Prototype floating spring-leg mechanism. (a) Front view. (b) Top view. The leg segments are of relatively equal length of 205 mm. The spring has a free length of approximately 114 mm and a force-deflection rate of 0.9 N/mm.

mechanical advantage between the spring and the leg, between each compression cycle.

2.5.2 Working principle

In this section we examine the working principle of the prototype shown in Fig. 2.5. Figure 2.6 shows the CAD model of the prototype, which features blue and orange colored parts to help distinguish which components are responsible for each endpoint of the spring assembly. As shown, each leg segment utilizes a pulley and dual cable assembly to move the endpoints of the spring assembly in unison.

During compression, see Fig. 2.6b-c, the spring is unlocked and applies force on the bearing-mounted endpoints of the spring. Subsequently, the ratchet and pawl lock the rotation of each pulley with respect to their associated knee bracket. This cable-pulley setup then locks the position of the endpoints against the force of the spring.

Following the spring compression, the spring is locked, and the pre-loaded retraction springs apply a torque on their respective pulleys, see Fig. 2.6d-e. Since the ratchet and pawl ensure the pulleys can only rotate in one direction, the torque on the pulley from the retraction spring tends to pull the endpoint of the spring assembly towards the knee joint. Therefore, as the mechanism returns to an initial configuration, the tension in the cables automatically shifts the endpoints of the spring towards the knee for a change in mechanical advantage before the next iteration.

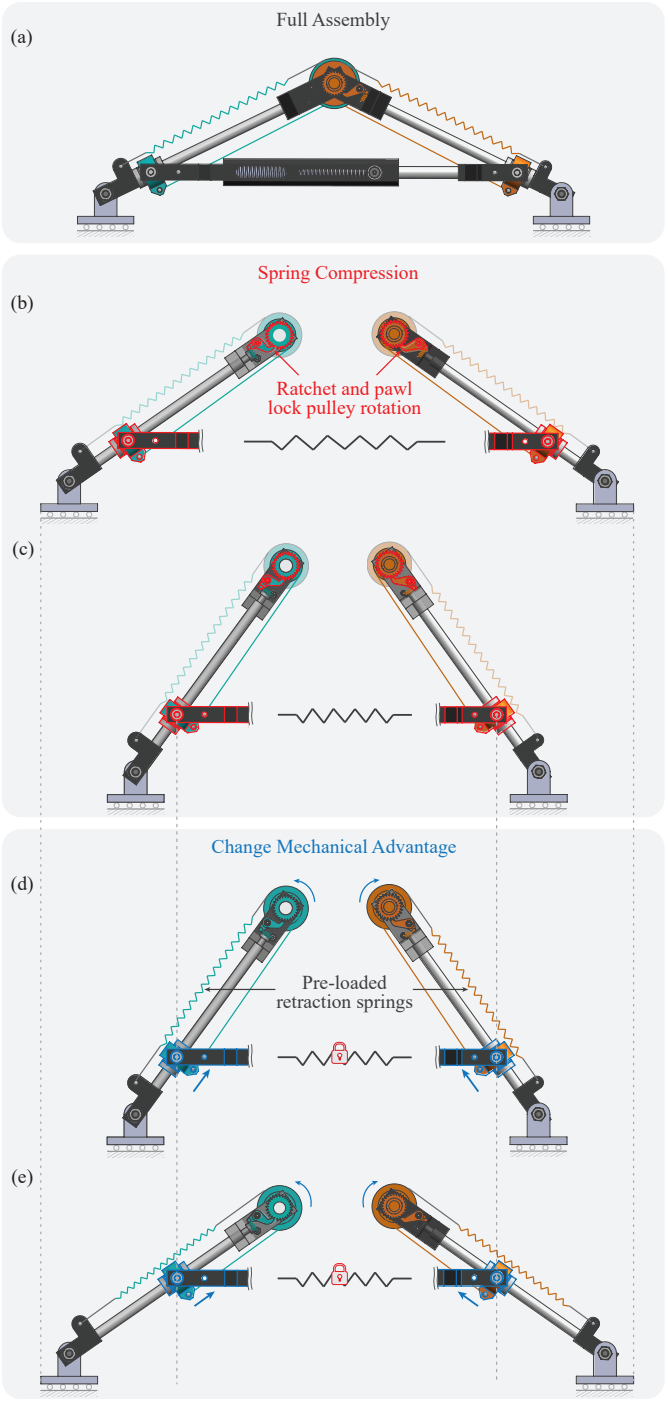

Figure 2.6: Compressing the spring and changing the mechanical advantage of the leg over the spring with the variable stiffness floating spring mechanism. (a) Front view of the CAD model. (b)-(c) Compressing the spring. During compression, the endpoints of the spring are fixed along the leg segments by locking the rotation of each respective pulley via a ratchet and pawl. (d)-(e) Changing the mechanical advantage of the leg over the spring. To change the mechanical advantage, the mechanism extends back to its initial configuration with the spring locked, allowing the pre-loaded retraction springs to rotate each pulley and simultaneously retract the spring endpoints towards the knee.

2.6 Experimental Validation

In this section, we use the prototype presented in Section 2.5 to evaluate the theoretical predictions shown in Fig. 2.4.

2.6.1 Experimental Setup

The prototype, shown in Fig. 2.5, was mounted on a mechanical breadboard via a linear rail. The ends of each leg segment were connected to lockable carriages. One carriage was locked in place, acting as the ankle joint fixing the foot of the mechanism to the ground, while the other carriage could move freely along the rail like the hip joint. A load cell (MLP-50, Transducer Techniques) was mounted to a flat plate on the free moving carriage to measure the force at the hip joint.

2.6.2 Experimental Procedure

To test the iterative energy accumulation process outlined in Section 2.4.2, the prototype was subject to the following experimental procedure.

First, with the spring unlocked, a force was applied to the load cell with constant velocity on the free slider until a pre-defined maximal force was reached. At that point, force was measured by the load cell. After collecting the force data, the spring was locked axially by tightening the friction clamp and the length of the spring was measured. Next, the slider was unlocked and moved back to its initial position. As described in Fig. 2.6d-e, moving the slider shifted the spring to a new configuration that granted greater mechanical advantage over the spring. The process described here was then repeated until maximum spring deformation was achieved.

2.6.3 Experimental Result

Figure 2.7 displays the experimental result.

Figure 2.7a, shows the force-deflection trend predicted in Section 2.4.2. Force is observed to increase up to the maximum force, then decrease to allow another squat despite the increased potential of the spring. The decrease in force required to enable a new squat is accomplished by the ratchet, pawl, and pulley assembly, described in Section 2.5.2. The iterative force-deflection behavior (solid lines) is compared to the force required to reach the same spring deflection in a single squat (dashed line).

Figure 2.7b shows the iterative increase in spring potential. The results show that the spring accumulates the same energetic potential in three squats (solid lines) as compared to that accumulated in one squat (dashed line). However, similar to what was predicted in Section 2.4.2, the mechanism reduces the amount of force necessary to accumulate the same amount of potential energy. In particular, the 25% decrease in

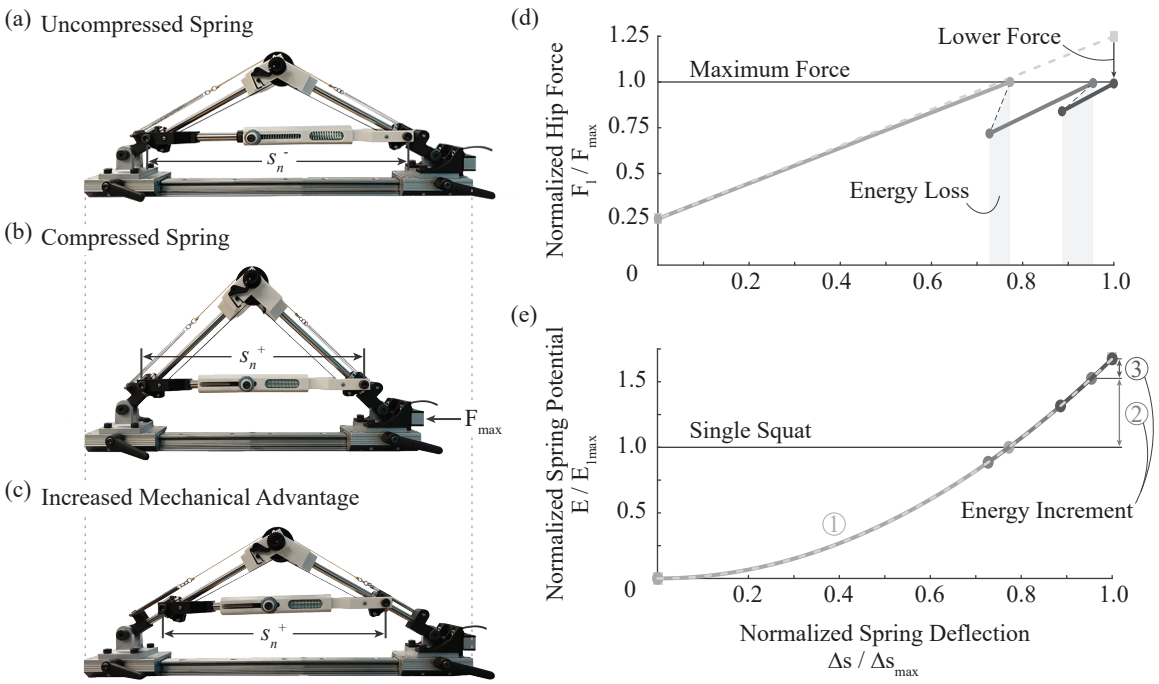

Figure 2.7: Experiment. (a)-(b) Example of one iteration performed during the experiment (solid lines in (d)). (c) Example of stiffness change between iterations (dashed lines in (d)). (d) Experimental force-deflection data for iterative energy accumulation using a limited force (solid lines). The data is normalized by the maximum force used to compress the spring. The maximum force is compared to the force required to achieve the same spring deflection after one compression (dashed line). (e) Experimental energy accumulation data, normalized by the maximum energy that can be accumulated in a single squat subject to maximum force (solid lines). The energy stored by the spring after three iterations with the limited force is compared to the energy that could be stored after one compression using a larger force (dashed line).

force observed in Fig. 2.7a resulted in 75% percent more energy accumulated by the spring compared to the energy one could store after a single squat when using the same maximal force. This result follows the same trend observed in Fig. 2.4. Further, when the device is reset to the initial mechanical advantage $x = l_t$, it yields nearly 25% more assistive force (Fig. 2.7a) and 75% more energy compared to the maximum force used to repetitively compress the spring and the associated energy stored by the spring when compressed by the maximum force in a single squat (Fig. 2.7b).

While the experimental results were similar to the theoretical predictions, there were notable differences. For example, the mechanism exhibited roughly 84 percent efficiency, due to the energy loss observed during the experiment. This energy loss is shown in Fig. 2.7a by the black dashed lines not being vertical between iterations. The loss of energy can also be observed in Fig. 2.7b, where the energy accumulated in the spring first decreased at the beginning of each new energy accumulation cycle.

Two main factors contributed to the observed energy loss; first, the cables used to couple the retraction springs to the spring assembly were not completely inextensible, and second, the ratchet and pawl only

provide discrete locking positions of the spring endpoints along the leg shafts, and therefore introduced some amount of backlash.

One can also observe in Fig. 2.7a that force is not initially zero, despite the zero initial spring potential, see Fig. 2.7b. This initial force was due to pre-loading of the compression spring to mitigate slack in the pulleys and cables. Also, the forces created by the retraction springs tend to pull the spring endpoints towards the knee, which in turn creates a moment about the knee that wants to straighten the leg.

2.7 Conclusion

In this paper, we studied a model of a human performing a repetitive squat-to-stand task to accumulate energy in a lower-limb spring-leg exoskeleton. This task was used as a representative example of iterative energy accumulation in a spring under force and deformation constraints. We proposed a variable stiffness floating spring leg mechanism to demonstrate the novel force-deflection and energy storage behavior conjectured in this study. Our theoretical predictions were experimentally validated using a prototype variable stiffness floating spring mechanism.

The prototype supplements the floating spring technology introduced in one of our prior works [28] by presenting a novel method for automatically adjusting the mechanical advantage of the human or a robot over a spring between compression iterations. The mechanism demonstrated the key novelty proposed in this work: a static gravitational force, provided by the mass of a human or robot, can be used to accumulate energy in a spring independent of the desired amount of energy stored by the spring.

The new capability of iterative energy accumulation using a limited static force, enabled by the method and device presented in this paper, could allow humans and robots with limited force capability and limited range of motion to perform physically demanding tasks, for example, to jump higher [25, 29, 20], move faster [30], or lift heavier objects [4], by harnessing the energy stored in assistive springs. The results presented in this work pave the way towards novel designs of robot exoskeletons and spring-driven robots with enhanced energy storage capabilities.

CHAPTER 3

Harnessing Accumulated Energy

So far, the focus has largely been on the method to accumulate energy. However, this chapter will explore how this accumulated energy can be harnessed to enhance performance in fundamental tasks, such as lifting and jumping.

For the proposed floating spring leg mechanism, releasing stored energy starts with shifting the spring to the initial configuration, $x = l_t$, to increase the mechanical advantage of the spring over the mass of the user. In Section 2.4.2, this resulted in over double the assistive force supplied to the user compared to the maximal force used to compress the spring. In turn, the user gains the potential to lift significantly more weight.

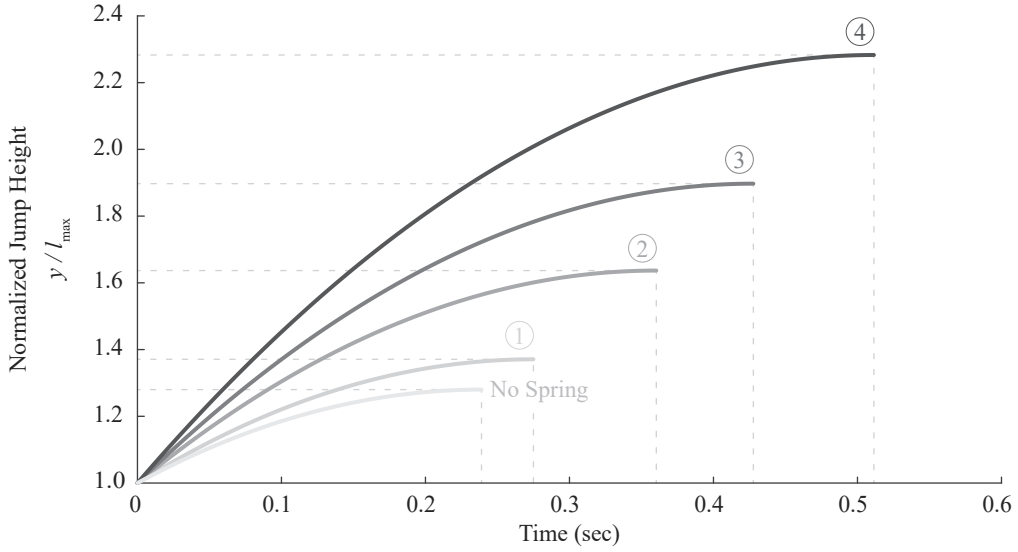

Figure 3.1: Comparison of achieved jump height with and without the assistive spring when releasing accumulated energy after one to four squat iterations.

Now, to investigate jumping, the ability of the legs is included together with the work done by the assistive spring during the motion. The average force of the legs is considered to be $1.7mg$ [25] and the mass of the user is considered a point mass. When released, the accumulated energy and the legs work to accelerate the mass until the legs are fully extended. Since $x = l_t$, Equation 2.7 asserts that $s = l$. In turn, the potential of the spring is completely transferred to kinetic energy of the mass at full leg extension. The velocity of the mass at takeoff can then be written as shown below, where s_f is the final compressed spring length after energy is

stored in the spring:

$$v = \left[\frac{k_s}{m} \left(s_{eq} - s_f \right)^2 + 1.4g \left(s_{eq} - s_f \right) \right]^{\frac{1}{2}}, \tag{3.1}$$

This kinetic energy then propels the user off the ground and, considering only the acceleration of gravity, simple analysis of constant acceleration expressions can be used to predict jump height. Figure 3.1 displays the maximum jump height achieved when accumulated energy is released after one or several compression iterations with the floating spring leg mechanism. Also, the jump heights achieved with the assistive spring are compared to the jump height reached when using the force of the legs alone.

Using this simple analysis, Figure 3.1 shows that iterative compressions enabled by the floating spring leg mechanism could yield jump heights over 50 percent higher than what could be achieved in a single iteration of energy storage and release using the same force to compress the spring, and nearly twice as high as the legs can do without spring assistance. Beyond increasing human jumping ability, this could prove useful in enabling increased jump heights in robots without an increase in motor size or power requirements.

CHAPTER 4

Discussion and Conclusion

This paper presented a novel method for iterative energy accumulation in assistive springs where the force to deform the spring can be independent from the energy stored by the spring (Section 2.4.2). Then, this method was demonstrated using a small scale prototype of a floating spring mechanism (Section 2.5.1). The key feature of the presented design was the ability to automatically adjust mechanical advantage between compression iterations while maintaining the potential energy of the spring (Section 2.4). While the feasibility of the proposed method was experimentally demonstrated on an initial prototype, this proof-of-concept was performed on a small scale tabletop mechanism. The ability to accumulate energy in assistive springs using bounded force and deformation on a broader scale poses several design challenges. To aid in the scalability of the proposed method for future designs, the rest of this chapter will delve further into key design considerations for the floating spring mechanism utilized in this work, and provide closing comments on this work as a whole.

4.1 Locking the Compression Spring

For this energy accumulation task, strategically adjusting stiffness between squats was necessary to allow the constant force provided by the weight of the user to continue to do work on the spring over repeated squats. While variable stiffness spring technology has a large body of work discussing the energetic benefit of adjustable impedance [31, 32, 33, 34, 35], the body of work narrows when considering mechanisms that allow adjustable impedance with maintained energetic potential [36, 28]. Such a behavior requires clutched-elastic actuation techniques using multiple clutches [6], with an ability to clutch and de-clutch the spring while under high forces from spring potential.

This work utilized independent clutching of the compression spring in the floating spring assembly, to lock the spring axially and maintain stored energy after each compression iteration, and the endpoints of the floating spring assembly, to automatically adjust stiffness between compression iterations. As detailed in Section 2.5.2, the working principle relied on a friction-based approach to achieve the necessary axially locking of the spring. While the friction clamp (see Fig. 2.5a) allowed infinite locking positions within the deformation range of the spring, the shoulder-bolt had to be manually tightened to secure the spring. This was an effective strategy for an initial proof of concept. However, ideally the working principle could be accomplished automatically during the repetitive compression procedure, much like how the stiffness adjustment occurs simultaneously with the movement of the mechanism back to its initial position.

Further, the required locking force increases proportionally with the energy stored by the spring, since the shoulder-bolt used in the friction clamp simply tightens to increase the normal force applied on the compression spring housing. To accomplish the same level of normal force without human input would require large or highly geared motors, adding significant weight to the floating spring assembly. To store significant energy on a human scale, as in Fig. 2.1, friction-based locking will require considerable forces to prevent slip [37], meaning the current approach may not be an efficient scalable solution.

Therefore, the ability to apply the energy accumulation method presented in this paper on a larger scale will benefit from spring designs that are lightweight, energy efficient, and capable of locking with minimal actuation force. This design challenge is an ongoing area of research. One promising solution that is being developed utilizes a capstan clutch to lock a compression spring at any deflection using small actuation force compared to the spring force.

4.2 Spring Retraction Assembly

As detailed in Section 2.5.1 and Section 2.5.2, the pulleys utilized in the floating spring assembly feature two drums rigidly connected to form a single body. One with a cable connecting to a bearing-supported endpoint of the spring, and the other with an oppositely wrapped cable connecting to an extension spring. In turn, the relative size of the drums determines the amount of force applied to the bearing, F_b, from the force of the extension spring, F_e. With D_b and D_e denoting the diameter of the bearing cable drum and extension cable drum (see Fig. 4.1b), respectively, the force of the extension spring and force on the bearing can be related:

$$F_b = F_e \left(\frac{D_e}{D_b} \right), \tag{4.1}$$

For the initial prototype, $D_e > D_b$ was selected to minimize the amount of extension spring force necessary to retract the compression spring assembly. With e denoting the length of the extension spring and k_e denoting the stiffness of the extension spring, the force of the extension spring can be written in terms of the diameters of the pulley drums, the pre-loaded length of the extension spring e_0, the equilibrium length of the extension spring e_{eq}, and the initial and current endpoint position of the compression spring assembly x_0 and x, respectively:

$$F_e = k_e \left(e_0 - e_{eq} \right) - k_e \left(\frac{D_e}{D_b} \right) \left(x_0 - x \right). \tag{4.2}$$

The first term represents the initial force of the extension spring due to pre-load, while the second term represents the decrease in force of the extension spring as the spring assembly retracts towards the knee.

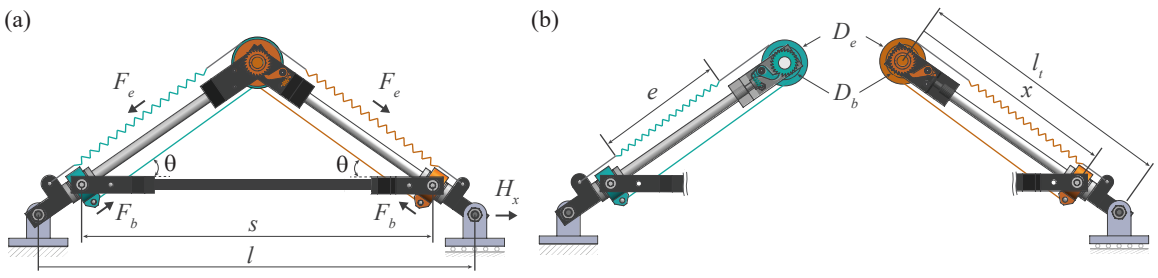

Figure 4.1: Force and kinematic analysis using the CAD model of the spring leg prototype. (a) With the compression spring locked, the floating spring assembly acts as a rigid link of length s. The force from the extension springs, F_e, creates a force F_b to retract the spring endpoint bearings towards the knee, which results in a force at the hip, H_x. (b) The extension springs, of length e, are coupled to the spring endpoint bearings by pulleys with two drums. The cable connected to the extension spring wraps around a drum of diameter D_e, while the cable connected to the spring endpoint bearing wraps around a drum of diameter D_b.

Also, as mentioned in Section 2.6.3, this system of pulleys and cables used to retract the compression spring assembly creates a non-negligible force at the hip that wants to straighten the mechanism (that is, increase the length of the mechanism, l). This force, denoted as H_x, arises from the retraction forces on the bearings:

$$H_x = F_b cos(\theta), \tag{4.3}$$

where,

$$cos(\theta) = \frac{s}{2x}. \tag{4.4}$$

From expression (4.3) and (4.4), H_x approaches F_b as x decreases and the endpoints of the spring approach the knee.

Further, Section 2.6.3 also mentioned how the discrete nature of the ratchet and pawl used in the spring retraction assembly contributed to the energy loss observed in the experimental results. Backlash between the ratchet and pawl means that, after being unlocked, the compression spring must extend slightly before the pawl engages with the ratchet and locks the motion of the spring endpoint bearings. Therefore, some of the energy stored by the spring is lost before force output from the mechanism is measured. For the initial proof-of-concept the ratchet and pawl were 3-D printed, meaning the ratchet teeth and tip of the pawl were limited by the minimum feature size achievable by the printer. To reduce backlash between the ratchet and pawl and increase the efficiency of the mechanism, future designs should utilize machined ratchet and pawl to achieve smaller pitch between the ratchet teeth and provide more continuous locking of the spring endpoint bearings along the leg shafts.

4.3 Conclusion

To improve the practicality of wearable assistive devices, such as exoskeletons and exosuits, researchers are faced with the challenge of efficiently utilizing energy in the human-exo system. Passive and quasi-passive assistive devices are a prominent solution to avoid large power supplies and motors that add significant weight and hinder desired functionality. However, passive assistive devices face several challenges before they can approach the versatility of active assistive devices. This paper outlined key theory and an initial prototype for a natural extension to passive exoskeleton technology: assistive devices that can accumulate energy in springs through repeated cycles of energy storage within the force and deformation limits of the human-wearable system.

The class of passive wearable assistive devices proposed in this work allow a limited force, like the weight of a user, to continue to do work on a spring despite increasing potential of the spring. Such devices rely on multiple clutches to independently control the energy stored by the spring and control the position of the spring in the mechanism to iteratively adjust the mechanical advantage between the applied force and the spring. It was also shown that this iterative change in mechanical advantage could be accomplished entirely passively, using a system of ratcheted pulleys and extension springs. Further, the importance of future work on lightweight and energy efficient designs to lock and store spring potential was discussed.

Appendix A

Psuedo-code

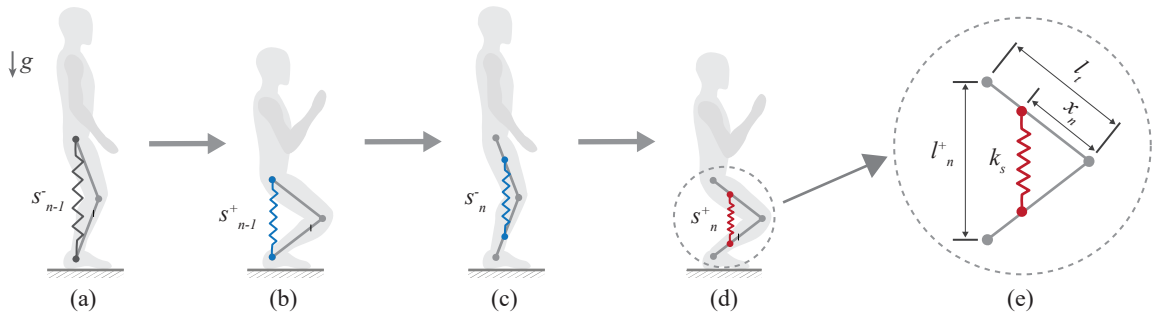

Figure A.1: (a)–(d) Iterative squat sequence with floating spring leg model. (e) Geometric parameters for the floating spring leg model.

Execute once using initial conditions:

Using moment balance about the knee, solve for initial compressed spring length:

$$mg = k_s \left(\frac{x_0}{l_t}\right)\left(s_{eq} - s_0^+\right) \Rightarrow s_0^+ = s_{eq} - \frac{mg}{k_s}\left(\frac{l_t}{x_0}\right) \tag{A.1}$$

Loop until: $\sum_{i=1}^{n} E_n = E_{desired} \;||\; s_n^+ = s_{min}$

Previous post-squat spring length retained as new pre-squat length:

$$s_n^- = s_{n-1}^+ \tag{A.2}$$

Apply similar triangles between Fig. A.1(a) and Fig. A.1(c) to determine new spring position:

$$x_n = \frac{s_n^-}{s_{n-1}^-} x_{n-1} \tag{A.3}$$

Using moment balance about the knee, solve for post-squat compressed spring length:

$$s_n^+ = s_{eq} - \frac{mg}{k_s}\left(\frac{l_t}{x_n}\right) \tag{A.4}$$

Analyze change in total energy:

$$\Delta E_n = \frac{1}{2} k_s \left[\left(s_{eq} - s_n^+\right)^2 - \left(s_{eq} - s_{n-1}^+\right)^2\right] \tag{A.5}$$

Determine post-squat leg length achieved, Fig. A.1(e):

$$l_n^+ = \left(\frac{l_t}{x_n}\right) s_n^+ \tag{A.6}$$

Update values for next loop:

$$s_{n-1}^+ = s_n^+; \quad s_{n-1}^- = s_n^-; \quad x_{n-1} = x_n \tag{A.7}$$

Appendix B

Matlab Code

Listing B.1: Script defines general parameters

```
function par = sl_parameters_vs()
persistent parameters
if isempty(parameters)
%% parameters
M = 50;              % point mass at the hip; kg
g = 9.81;            % accel. due to gravity; m/s^2
l_t = 0.525;         % thigh length; m
l_sh = 0.525;        % shank length; m
y_max = 1.0;         % initial hip height; m
y_min = 0.60*y_max; % minimum hip height; m
s_eq = y_max;        % spring equilibrium length; m
s_min = 0.3*s_eq;    % minimum spring length; m
%% store in parameters variable
parameters.M = M;
parameters.g = g;
parameters.lt = l_t;
parameters.lsh = l_sh;
parameters.ymax = y_max;
parameters.ymin = y_min;
parameters.s_eq = s_eq;
parameters.smin = s_min;
end
par = parameters;
end
```

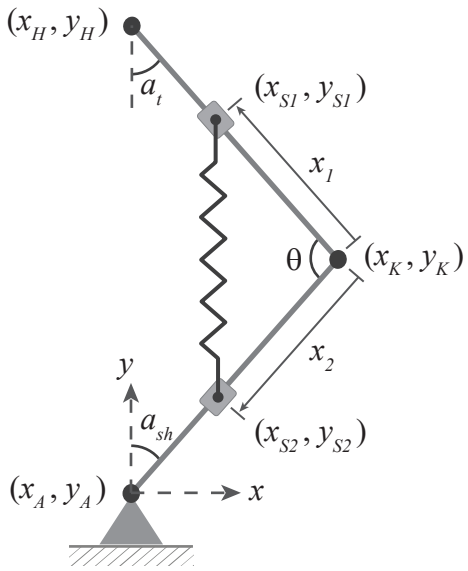

Figure B.1: Spring leg geometry defined in terms of lab frame coordinates.

Listing B.2: Script outputs leg coordinates as defined by Figure B.1

```
function [xS1,yS1,xS2,yS2,xK,yK] = resolve_coord(x,y_in)
%% Import parameters
par = sl_parameters_vs();
l_t = par.lt;
l_sh = par.lsh;
%% Calculate leg angles
%relative angle between thigh and shank leg segments
theta_in = acos((l_t.^2 + l_sh.^2 - y_in.^2)./(2.*l_t.*l_sh));
%thigh angle from the vertical
a_t = asin((l_sh./y_in).*sin(theta_in));
%shank angle from the vertical
a_sh = pi - theta_in - a_t;
%% Evaluate joint positions in lab frame coordinates
x1_temp = l_t - x;  %distance from hip to thigh endpoint position
x2_temp = l_sh - x; %distance from ankle to shank endpoint position
xK = l_sh.*sin(a_sh); yK = l_sh.*cos(a_sh);
xS1 = x1_temp.*sin(a_t); yS1 = y_in - x1_temp.*cos(a_t);
xS2 = x2_temp.*sin(a_sh); yS2 = x2_temp.*cos(a_sh);
```

Listing B.3: Script runs main simulation

```
clear; clc; close all;
```

```
%% Import parameters
par = sl_parameters_vs();
M = par.M;
l_t = par.lt;
l_sh = par.lsh;
y_max = par.ymax;
y_min = par.ymin;
s_eq = par.s_eq;
s_min = par.smin;
g = par.g;
```

```
%% Determine key constants
F_max = M*g;
dely_max = y_max - y_min;
W_max = F_max*dely_max;
E_desired = 1.75*W_max;
k_min = (2*E_desired)/(s_eq - s_min)^2;
k_0 = 1.1325*k_min; %selected to prioritize full squats
s_init = s_eq - F_max/k_0; %spring length after initial deflection
s_prevPlus = s_init; %initial compressed spring length achieved
s_prevMinus = s_eq;  %initial spring length before first compression
x_iPrev = l_t;
%define figures
leg_fig = figure;    %plot hip force v. leg deflection
spring_fig = figure; %plot hip force v. spring deflection
E_fig = figure;      %plot spring potential v. spring deflection
n = 0; %track number of iterations
sfail_flag = 1; %initialize error flag
```

```
%% Initialize arrays
x_array = 0;
xK_mat = [];  yK_mat = [];
```

```
xS1_mat = []; yS1_mat = [];
xS2_mat = []; yS2_mat = [];
xH = 0; yH_mat = [];
xA = 0; yA = 0;
Fout_mat = [];
sout_mat = [];
s_lengths_array = [];
s_array = s_init;
ycomp_array = (l_t/x_iPrev)*s_init;
sdef_array = [0 s_eq-s_init];
ydef_array = [0 y_max-ycomp_array];
```

```
%% Calculate leg coordinates for initial squat
y_temp = linspace(y_max,ycomp_array);
yH_mat = horzcat(yH_mat,y_temp);

[xS1,yS1,xS2,yS2,xK,yK] = resolve_coord(x_iPrev,y_temp);

xK_mat = horzcat(xK_mat, xK); yK_mat = horzcat(yK_mat, yK);
xS1_mat = horzcat(xS1_mat, xS1); yS1_mat = horzcat(yS1_mat, yS1);
xS2_mat = horzcat(xS2_mat, xS2); yS2_mat = horzcat(yS2_mat, yS2);
```

```
%% Plot initial force-deflection
y_input = linspace(y_max,ycomp_array);
def_temp = y_max - y_input;
F_out = k_0.*def_temp;
Fout_mat = horzcat(Fout_mat,F_out);
sout_mat = horzcat(sout_mat,(x_iPrev/l_t).*y_input);
figure(leg_fig)
plot(def_temp,F_out./F_max) %Normalized
figure(spring_fig)
plot([0,(s_eq - s_init)./(s_eq - s_min)],[0,F_max./F_max]) %Normalized
```

```
%% Main loop
while sfail_flag > 0
```

```
    n = n + 1;
    %set a bound on the number of iterations
    if n > 20
        disp('loop iteration limit reached')
        break
    end
%%Solve for x_i to satisfy initial geometry each iteration
    s_iMinus = s_prevPlus;
    x_i = (s_iMinus/s_prevMinus)*(x_iPrev);
%%Calculate leg coordinates for shift of x_iPrev to x_i as previous iteration
    returns to standing
    x_temp = linspace(x_iPrev,x_i);
    y_temp = linspace(ycomp_array(n),y_max);
    yH_mat = horzcat(yH_mat,y_temp);

    [xS1,yS1,xS2,yS2,xK,yK] = resolve_coord(x_temp,y_temp);

    xK_mat = horzcat(xK_mat, xK); yK_mat = horzcat(yK_mat, yK);
    xS1_mat = horzcat(xS1_mat, xS1); yS1_mat = horzcat(yS1_mat, yS1);
    xS2_mat = horzcat(xS2_mat, xS2); yS2_mat = horzcat(yS2_mat, yS2);
    %%update force and spring arrays for the shift
    Fout_mat = horzcat(Fout_mat,Fout_mat(end).*ones(1,100));
    sout_mat = horzcat(sout_mat,sout_mat(end).*ones(1,100));
%%Form deformation expressions
    s_iPlus = s_eq - (l_t/(k_0*x_i))*M*g; %compressed spring length
    y_ii = (l_t/x_i)*s_iPlus; %new minimum mass height
    def_yii = y_max - y_ii;
%%Update arrays
    s_lengths_array = cat(2,s_lengths_array,s_prevPlus,s_iPlus);
    ydef_array = cat(2,ydef_array,def_yii);
    sdef_array = cat(2,sdef_array,(s_eq - s_iPlus));
    s_array = cat(2,s_array,s_iPlus);
```

```
    ycomp_array = cat(2,ycomp_array,y_ii);
%%Calculate and plot output force-deflection behavior each iteration
    y_input = linspace(y_max,y_ii,1000);
    def_temp = y_max - y_input;
    s_out = (x_i./l_t).*y_input; %calculate spring length
    F_out = (x_i./l_t).*k_0.*(s_eq - s_out); %calculate hip force
    %%Check that s_out does not surpass s_min
    if any(s_out <= s_min)
        disp('Error: sol_s < s_min, hard stop reached!')
        [~,sfail_index] = min(abs(s_out-s_min));
        F_out = F_out(1:sfail_index); %trim Force output up to s_min
        s_out = s_out(1:sfail_index); %trim s length vector up to s_min
        sfail_flag = -1;              %set flag < 0
        sdef_array(end) = (s_eq - s_out(sfail_index));
        s_array(end) = s_out(sfail_index);
        def_temp = def_temp(1:sfail_index); %trim vector up to s_min index
        ycomp_array(end) = y_input(sfail_index);
    end %end error checking
%%Save force and spring deformation arrays (must maintain consistent array size)
    Fout_mat = horzcat(Fout_mat,linspace(F_out(1),F_out(end)));
    sout_mat = horzcat(sout_mat,linspace(s_out(1),s_out(end)));
%%Calculate leg coordinates for current iteration with x_i and y_max to y_ii
    y_temp = linspace(y_max,ycomp_array(end));
    yH_mat = horzcat(yH_mat,y_temp);

    [xS1,yS1,xS2,yS2,xK,yK] = resolve_coord(x_i,y_temp);

    xK_mat = horzcat(xK_mat, xK);
    yK_mat = horzcat(yK_mat, yK);
    xS1_mat = horzcat(xS1_mat, xS1);
    yS1_mat = horzcat(yS1_mat, yS1);
    xS2_mat = horzcat(xS2_mat, xS2);
```

```
    yS2_mat = horzcat(yS2_mat, yS2);
%%Plot force-deflection result for current iteration
    figure(leg_fig)
    hold on
    plot(def_temp./dely_max,F_out./F_max) %Normalized
    figure(spring_fig)
    hold on
    plot((s_eq - s_out)./(s_eq - s_min),F_out./F_max) %Normalized
%%Calculate relative energy change
    E_ch = abs(0.5*k_0*(s_eq - s_prevPlus)^2 - 0.5*k_0*(s_eq - s_iPlus)^2);
    E_ch_norm = E_ch./W_max;
%%Update values
    s_prevPlus = s_iPlus; s_prevMinus = s_iMinus; x_iPrev = x_i;
end %end Main loop
```

```
%% Add figure labels
figure(leg_fig)
title('Force v. Deflection');
xlabel('Output/Mass Height Deflection (m)');
ylabel('Mechanism Output Force')
figure(spring_fig)
title('Normalized Output Force v. Spring Deflection');
xlabel('Spring Deflection (m)'); ylabel('Normalized Output Force')
```

```
%% Plot PE behavior - Normalized by E_max from single squat at k_0
E_total_array = 0.5.*k_0.*(sdef_array).^2; %potential after n iterations
E_max = 0.5*k_0*(sdef_array(2))^2 - 0.5*k_0*(sdef_array(1))^2;
figure(E_fig)
hold on
def_temp = linspace(0,s_eq - s_min);
E_temp = 0.5.*k_0.*(def_temp).^2;
plot(def_temp./(s_eq - s_min),E_temp./E_max,'LineWidth',2)
title('Spring Potential v. Spring Deformation')
xlabel('Deflection (m)')
```

```
ylabel('Normalized Spring Potential')
yticks(0:0.25:5.25)
xlim([0 1])
%Add horizontal lines to segment each energy accumulation iteration
for i = 2:length(E_total_array)
    yline(E_total_array(i)./E_max,'--',sprintf('n = %d',i-1))
end
```

```
%% Plot single squat & 3 squat - Normalized
figure(spring_fig)
plot([0 s_eq - s_min]./(s_eq - s_min),[0 k_0*(s_eq - s_min)]./F_max)
ylim([0 2.3])
yticks(0:0.25:2.25)
```

```
%% Animate
xA_mat = zeros(1,length(xK_mat)); yA_mat = zeros(1,length(xK_mat));
xH_mat = zeros(1,length(xK_mat));
itemp = 1;
f_animate = figure();
f_animate.WindowState = 'maximized';
for i = 1:length(yH_mat)
%%Spring Leg Motion
    sub = subplot(2,3,[1,4]);
    cla(sub); hold on;
    xline(0,':') %draw line along the mass deflection
    %draw the shank leg segment
    line([xA_mat(i) xK_mat(i)],[yA_mat(i) yK_mat(i)],...
        'Color','k','LineWidth',3,'Marker','.','MarkerSize',24)
    %draw the thigh leg segment
    line([xK_mat(i) xH_mat(i)],[yK_mat(i) yH_mat(i)],...
        'Color','k','LineWidth',3,'Marker','.','MarkerSize',24)


    %plot the spring
    t = 0:0.01:1;
```

```
spring_offset = 0.15;
ss = (yS1_mat(i) - yS2_mat(i)) - spring_offset; %set length of spring
t = ss*t;
freq = 8/ss; %influence number of spring coils
Rot = [cosd(-90), -sind(-90); sind(-90), cosd(-90)]; %set orientation
springs = Rot*[t; 0.025*sin(2*pi*freq*t)];
plot(springs(1,:)+xS1_mat(i),springs(2,:)+yS1_mat(i)-spring_offset/2,...
    'Color',[0.3 0.3 0.3],'LineWidth',2) %draw the spring
line([xS1_mat(i) xS2_mat(i)],[yS1_mat(i) yS1_mat(i)-spring_offset/2],...
    'Color',[0.3 0.3 0.3],'LineWidth',2) %draw the spring offset
line([xS1_mat(i) xS2_mat(i)],[yS2_mat(i) yS2_mat(i)+spring_offset/2],...
    'Color',[0.3 0.3 0.3],'LineWidth',2) %draw the spring offset
%draw spring endpoint slider; change color based on locked/unlocked
if i > 100 && i < 200
    plot(xS1_mat(i),yS1_mat(i),'b.','MarkerSize',24)
    plot(xS2_mat(i),yS2_mat(i),'b.','MarkerSize',24)
elseif i > 300 && i < 400
    plot(xS1_mat(i),yS1_mat(i),'b.','MarkerSize',24)
    plot(xS2_mat(i),yS2_mat(i),'b.','MarkerSize',24)
elseif i > 500 && i < 600
    plot(xS1_mat(i),yS1_mat(i),'b.','MarkerSize',24)
    plot(xS2_mat(i),yS2_mat(i),'b.','MarkerSize',24)
else
    plot(xS1_mat(i),yS1_mat(i),'r.','MarkerSize',24)
    plot(xS2_mat(i),yS2_mat(i),'r.','MarkerSize',24)
end

%plot the mass at the hip
plot(0, yH_mat(i),'Color',[0.5 0.5 0.5],'Marker','.','MarkerSize',150);
text(xH_mat(i),yH_mat(i),'M','HorizontalAlignment','center',...
    'FontSize',20)
hold off
```

```
    axis([-0.5 0.5 0 1.5])
    drawnow
%%Force v. Deflection
    sub2 = subplot(2,3,[2,3]);
    xlabel('Normalized Spring Deflection','FontSize',14)
    ylabel('Normalized Hip Force','FontSize',14)
    hold on
    axis([0 1 0 max(Fout_mat./F_max)])
    %define color factor (cf), line width (lw), and line style (ls) for
    %each section of force deflection profile
    if i <= 100
        cf = 0.8;
        lw = 3; ls = '-';
    elseif i>200 && i <=201 %insert dashed vertical line
        itemp = 200;
        cf = 0.1;
        lw = 1; ls = '--';
    elseif i>201 && i <= 300
        itemp = 202;
        cf = 0.6;
        lw = 3; ls = '-';
    elseif i>400 && i <= 401 %insert dashed vertical line
        itemp = 400;
        cf = 0.1;
        lw = 1; ls = '--';
    elseif i>401 && i <= 500
        itemp = 402;
        cf = 0.4;
        lw = 3; ls = '-';
    elseif i>600 && i <= 601 %insert dashed vertical line
        itemp = 600;
        cf = 0.1;
```

```
        lw = 1; ls = '--';
    elseif i <= 700
        itemp = 602;
        cf = 0.2;
        lw = 3; ls = '-';
    end
    plot((s_eq - sout_mat(itemp:i))./(s_eq - s_min),...
        (Fout_mat(itemp:i))./F_max,...
        'Color',[cf cf cf],'LineWidth',lw,'LineStyle',ls)
%%Potential v. Deflection
    sub3 = subplot(2,3,[5,6]);
    xlabel('Normalized Spring Deflection','FontSize',14)
    ylabel('Normalized Spring Potential','FontSize',14)
    hold on
    axis([0 1 0 max(E_total_array./E_max)])
    if i <= 100
        cf = 0.8;
    elseif i>100 && i <= 300
        itemp = 100;
        cf = 0.6;
    elseif i>300 && i <= 500
        itemp = 300;
        cf = 0.4;
    elseif i <= 700
        itemp = 500;
        cf = 0.2;
    end
    plot((s_eq - sout_mat(itemp:i))./(s_eq - s_min),...
        (0.5.*k_0.*(s_eq - sout_mat(itemp:i)).^2)./E_max,...
        'Color',[cf cf cf],'LineWidth',3)
    movieVector(i) = getframe(gcf);
end %end Animation loop
```

```
%% Save the animation as a mp4 video
myWriter = VideoWriter('LegMotion', 'MPEG-4');
myWriter.FrameRate = 20;
open(myWriter);
writeVideo(myWriter, movieVector);
close(myWriter);
```

```
%% Determine jump behavior - solve projectile dynamics
figure
%plot jump height achieved by leg force alone
v_leg = sqrt(1.4*g*(y_max - y_min));
%time to reach peak height
t_peak = v_leg/g;
tspan_peak = linspace(0,t_peak,100);
%calculate peak height
y_peak = y_max + v_leg.*tspan_peak - 0.5.*g.*tspan_peak.^2;
hold on
plot(tspan_peak,y_peak./y_max)
for i = 1:length(s_array)
    %calculate takeoff velocity
    v_off = sqrt((k_0/M)*(s_eq - s_array(i))^2 +...
        1.4*g*(y_max - s_array(i)));
    %time to reach peak height
    t_peak = v_off/g;
    tspan_peak = linspace(0,t_peak,100);
    %calculate peak height
    y_peak = y_max + v_off.*tspan_peak - 0.5.*g.*tspan_peak.^2;
    plot(tspan_peak,y_peak./y_max)
end
```

References

[1] Aaron J. Young and Daniel P. Ferris. State of the art and future directions for lower limb robotic exoskeletons. *IEEE Transactions on Neural Systems and Rehabilitation Engineering*, 25(2):171–182, 2017.

[2] Longhan Xie, Guowei Huang, Ledeng Huang, Siqi Cai, and Xiaodong Li. An unpowered flexible lower limb exoskeleton: Walking assisting and energy harvesting. *IEEE/ASME Transactions on Mechatronics*, 24(5):2236–2247, 2019.

[3] Tiancheng Zhou, Caihua Xiong, Juanjuan Zhang, Wenbin Chen, and Xiaolin Huang. Regulating metabolic energy among joints during human walking using a multiarticular unpowered exoskeleton. *IEEE Transactions on Neural Systems and Rehabilitation Engineering*, 29:662–672, 2021.

[4] Erik P. Lamers, Aaron J. Yang, and Karl E. Zelik. Feasibility of a biomechanically-assistive garment to reduce low back loading during leaning and lifting. *IEEE Transactions on Biomedical Engineering*, 65(8):1674–1680, 2018.

[5] Steven H. Collins, M. Bruce Wiggin, and Gregory S. Sawicki. Reducing the energy cost of human walking using an unpowered exoskeleton. *Nature*, 522(7555):212–215, 2015.

[6] Michiel Plooij, Wouter Wolfslag, and Martijn Wisse. Clutched elastic actuators. *IEEE/ASME Transactions on Mechatronics*, 22(2):739–750, apr 2017.

[7] Daniel Paluska and Hugh Herr. The effect of series elasticity on actuator power and work output: Implications for robotic and prosthetic joint design. *Robotics and Autonomous Systems*, 54(8):667–673, 2006.

[8] David J. Braun, Vincent Chalvet, Tze Hao Chong, Salil S. Apte, and Neville Hogan. Variable stiffness spring actuators for low-energy-cost human augmentation. *IEEE Transactions on Robotics*, 35(6):1435–1449, 2019.

[9] David J. Braun, Florian Petit, Felix Huber, Sami Haddadin, Patrick van der Smagt, Alin Albu-Schäffer, and Sethu Vijayakumar. Robots driven by compliant actuators: Optimal control under actuation constraints. *IEEE Transactions on Robotics*, 29(5):1085–1101, 2013.

[10] Michiel Plooij, Martijn Wisse, and Heike Vallery. Reducing the energy consumption of robots using the bidirectional clutched parallel elastic actuator. *IEEE Transactions on Robotics*, 32(6):1512–1523, 2016.

[11] Hung Quy Vu, Xiaoxiang Yu, Fumiya Iida, and Rolf Pfeifer. Improving energy efficiency of hopping locomotion by using a variable stiffness actuator. *IEEE/ASME Transactions on Mechatronics*, 21(1):472–486, 2016.

[12] Anirban Mazumdar, Steven J. Spencer, Clinton Hobart, Jonathan Salton, Morgan Quigley, Tingfan Wu, Sylvain Bertrand, Jerry Pratt, and Stephen P. Buerger. Parallel elastic elements improve energy efficiency on the STEPPR bipedal walking robot. *IEEE/ASME Transactions on Mechatronics*, 22(2):898–908, 2017.

[13] Hendrik Kolvenbach, Elias Hampp, Patrick Barton, Radek Zenkl, and Marco Hutter. Towards jumping locomotion for quadruped robots on the moon. In *2019 IEEE/RSJ International Conference on Intelligent Robots and Systems (IROS)*, pages 5459–5466, Macau, China, Nov. 2019.

[14] Kevin W. Hollander, Robert Ilg, Thomas G. Sugar, and Donald Herring. An efficient robotic tendon for gait assistance. *Journal of Biomechanical Engineering*, 128(5):788–791, 2006.

[15] Shiqian Wang, Wietse Van Dijk, and Herman Van Der Kooij. Spring uses in exoskeleton actuation design. *IEEE International Conference on Rehabilitation Robotics*, pages 6–11, 2011.

[16] David J. Braun, Salil S. Apte, Olzhas Adiyatov, Abhinav Dahiya, and Neville Hogan. Compliant actuation for energy efficient impedance modulation. In *2016 IEEE International Conference on Robotics and Automation (ICRA)*, pages 636–641, Stockholm, Sweden, May 2016.

[17] Amanda Sutrisno and David J. Braun. How to run 50% faster without external energy. *Science Advances*, 6(13):1–11, 2020.

[18] Wonseok Shin, Gunhee Park, Jooyong Lee, Handdeut Chang, and Jung Kim. Power transmission design of fast and energy-efficient stiffness modulation for human power assistance. In *2021 IEEE International Conference on Robotics and Automation (ICRA)*, pages 10877–10883, Xi'an, China, May-June 2021.

[19] Cunjin Wang, Lei Dai, Donghua Shen, Jiyuan Wu, Xingsong Wang, Mengqian Tian, Yunde Shi, and Chun Su. Design of an ankle exoskeleton that recycles energy to assist propulsion during human walking. *IEEE Transactions on Biomedical Engineering*, 69(3):1212–1224, 2022.

[20] Elliot W. Hawkes, Charles Xiao, Richard Alexandre Peloquin, Christopher Keeley, Matthew R. Begley, Morgan T. Pope, and Günter Niemeyer. Engineered jumpers overcome biological limits via work multiplication. *Nature*, 604:657–661, 2022.

[21] O.H. Okubo, Eiji Nakano, and M. Handa. Design of a jumping machine using self-energizing spring. volume 1, pages 186–191, Osaka, Japan, Nov. 1996.

[22] David J. Braun, Matthew Howard, and Sethu Vijayakumar. Exploiting variable stiffness in explosive movement tasks. In *Proceedings of Robotics: Science and Systems*, Los Angeles, CA, USA, June-July 2011.

[23] Alexandra Velasco, Manolo Garabini, Manuel G. Catalano, and Antonio Bicchi. Soft actuation in cyclic motions: Stiffness profile optimization for energy efficiency. In *2015 IEEE-RAS 15th International Conference on Humanoid Robots (Humanoids)*, pages 107–113, Seoul, Korea (South), Nov. 2015.

[24] Duncan W. Haldane, M. M. Plecnik, J. K. Yim, and R. S. Fearing. Robotic vertical jumping agility via Series-Elastic power modulation. *Science Robotics*, 1(1):eaag2048, 2016.

[25] Amanda Sutrisno and David J. Braun. Enhancing mobility with quasi-passive variable stiffness exoskeletons. *IEEE Transactions on Neural Systems and Rehabilitation Engineering*, 27(3):487–496, 2019.

[26] Chase W. Mathews and David J. Braun. Design of parallel variable stiffness actuators. *IEEE Transactions on Robotics*, pages 1–15, 2022.

[27] George B. Hansburg. Pogo stick, U.S. Patent 2 793 036 May 21, 1957.

[28] Sung Y. Kim and David J. Braun. Novel variable stiffness spring mechanism: Modulating stiffness independent of the energy stored by the spring. *IEEE International Conference on Intelligent Robots and Systems*, pages 8232–8237, 2021.

[29] Philip Arm, Radek Zenkl, Patrick Barton, Lars Beglinger, Alex Dietsche, Luca Ferrazzini, Elias Hampp, Jan Hinder, Camille Huber, David Schaufelberger, Felix Schmitt, Benjamin Sun, Boris Stolz, Hendrik Kolvenbach, and Marco Hutter. Spacebok: A dynamic legged robot for space exploration. In *2019 International Conference on Robotics and Automation (ICRA)*, pages 6288–6294, Montreal, QC, Canada, May 2019.

[30] Tiange Zhang and David J. Braun. Theory of fast walking with human-driven load-carrying robot exoskeletons. *IEEE Transactions on Neural Systems and Rehabilitation Engineering*, 30:1971–1981, 2022.

[31] Chad English and Donald L. Russell. Mechanics and stiffness limitations of a variable stiffness actuator for use in prosthetic limbs. *Mechanism and Machine Theory*, 34(1):7–25, 1999.

[32] Van Ronald Ham, Thomas G. Sugar, Bram Vanderborght, Kevin W. Hollander, and Dirk Lefeber. Compliant actuator designs: Review of actuators with passive adjustable compliance/controllable stiffness for robotic applications. *IEEE Robotics and Automation Magazine*, 16(3):81–94, 2009.

[33] Sebastian Wolf, Giorgio Grioli, Oliver Eiberger, Werner Friedl, Markus Grebenstein, Hannes Höppner, Etienne Burdet, Darwin G. Caldwell, Raffaella Carloni, Manuel G. Catalano, Dirk Lefeber, Stefano Stramigioli, Nikos Tsagarakis, Michaël Van Damme, Ronald Van Ham, Bram Vanderborght, Ludo C. Visser, Antonio Bicchi, and Alin Albu-Schäffer. Variable stiffness actuators: Review on design and components. *IEEE/ASME Transactions on Mechatronics*, 21(5):2418–2430, 2016.

[34] Chase W. Mathews and David J. Braun. Parallel variable stiffness actuators. In *2021 IEEE/RSJ International Conference on Intelligent Robots and Systems (IROS)*, pages 8225–8231, 2021.

[35] Tiange Zhang and David J. Braun. Human driven compliant transmission mechanism. In *2021 IEEE International Conference on Robotics and Automation (ICRA)*, pages 7094–7099, 2021.

[36] Ludo C. Visser, Raffaella Carloni, and Stefano Stramigioli. Energy-efficient variable stiffness actuators. *IEEE Transactions on Robotics*, 27(5):865–875, 2011.

[37] Michiel Plooij, Glenn Mathijssen, Pierre Cherelle, Dirk Lefeber, and Bram Vanderborght. Lock your robot: A review of locking devices in robotics. *IEEE Robotics and Automation Magazine*, 22(1):106–117, 2015.